Endocytosis of peroxiredoxin 1 links sterile inflammation to immunoparalysis in pediatric patients following cardiopulmonary bypass

Chia-Hsiung Liu [a,b], Zheng-Hua Huang [b], Shu-Chien Huang [b,*], Tzuu-Shuh Jou [a,c,d,**]

[a] Graduate Institute of Clinical Medicine, College of Medicine, National Taiwan University, Taipei, Taiwan
[b] Department of Surgery, College of Medicine, National Taiwan University, Taipei, Taiwan
[c] Department of Internal Medicine, National Taiwan University Hospital, Taiwan
[d] Center of Precision Medicine, College of Medicine, National Taiwan University, Taiwan

ABSTRACT

After cardiopulmonary bypass (CPB), the occurrence of systemic inflammatory response is often accompanied by a persistent compensatory anti-inflammatory response syndrome that can lead to a compromised immune competence termed immunoparalysis, rendering the patients susceptible to infections which is a leading complication following cardiac surgery. However, the underlying mechanisms of CPB-elicited immunoparalysis remain obscure. In this study we showed that peroxiredoxin 1 (Prdx1), a putative cytosolic antioxidant, was released immediately after CPB in a cohort of pediatric patients receiving congenital cardiac surgery. This increased Prdx1 was correlated to a reduced human leukocyte antigen-DR expression and an elevated interleukin-10 (IL-10) production, as well as a hypo-responsiveness of macrophages to endotoxin and a higher incidence of nosocomial infection. We demonstrated that substitution of Ser^{83} for Cys^{83} prevented Prdx1 from oligomerization and subsequent binding and internalization to macrophages. These effects mitigated Prdx1-induced IL-10 induction and endotoxin tolerance. Furthermore, after engagement with toll-like receptor (TLR) 4, clathrin-dependent endocytosis is crucial for Prdx1 to elicit IL-10 production in phagocytes. Congruently, inhibition of Prdx1/TLR4 endocytosis in phagocytes reversed the Prdx1/IL-10-mediated hypo-responsiveness to endotoxin. Our findings unveiled the possible mechanisms by which Prdx1 undertakes to cause immunoparalysis, and targeting endocytosis of Prdx1 could be a novel therapeutic approach for postoperative infections associated with CPB.

1. Introduction

It is well documented that drastic hemodynamic situations such as severe trauma or cardiopulmonary bypass (CPB) procedure associated with cardiac surgery can elicit production and release of numerous pro-inflammatory mediators by the innate immune system [1–3]. This systemic inflammatory response syndrome (SIRS) is accompanied by a compensatory anti-inflammatory response syndrome (CARS) aiming to restore homeostasis. However, a prolonged or exaggerated CARS often leads to a status of marked reduction in immune competence known as immune tolerance or immunoparalysis, rendering the host susceptible to infections [4]. Compared to SIRS, the pathogenesis and critical causative molecular mediators of CARS are far less understood.

Immunoparalysis can be quantified through the measurement of monocytic human leukocyte antigen (HLA)-DR expression or via analysis of the *ex vivo* capacity of blood leukocytes to produce tumor necrosis factor (TNF)-α upon stimulation with endotoxin [4,5]. Several studies have demonstrated that CPB induced immunoparalysis following pediatric heart surgery, and elevation of anti-inflammatory cytokine interleukin-10 (IL-10) plays a pivotal role in the pathogenesis [6–8]. However, the underlying mechanism leading to dysregulation of IL-10 production under CPB or other perturbing hemodynamic conditions remains poorly understood.

Pattern recognition receptors such as toll like receptor 4 (TLR4) could recognize molecular patterns of intrinsic host materials which are released during hypoxia and ischemia-related cell injury or death, the

so-called damage-associated molecular patterns (DAMPs), to provoke severe sepsis-like syndrome [9–11]. In patients with cardiac arrest and trauma, the increased plasma levels of DAMPs are associated with the development of immunoparalysis [12,13]. It has been recently demonstrated that IL-10 signaling pathway plays an instrumental role in myeloid-related proteins (MRPs)-induced phagocyte hypo-responsiveness to endotoxin in a group of patients with CPB-elicited sterile inflammation [14]. Although these findings support a causative link between MRPs and IL-10 in innate immune tolerance, it remains unsolved whether other DAMP is involved in CPB-induced immunoparalysis and IL-10 may play a similar role under such situation.

The newly identified DAMP Peroxiredoxin 1 (Prdx1) is a ubiquitous antioxidant possessing peroxidase and chaperon-like activities intracellularly [15–18]; nevertheless, when released extracellularly under various pathological situations, Prdx1 becomes a noxious promoter of inflammation, which interacts with innate immune receptors to induce the expression of pro-inflammatory cytokines, and thereby, initiates acute sterile inflammation [19–23]. We have discovered that circulating Prdx1 prognosticates the severity of SIRS in patients with cardiogenic shock receiving extracorporeal membrane oxygenation support, and the plasma IL-10 levels are positively correlated to the levels of plasma Prdx1 in this cohort of patients [24]. These data denote that Prdx1 may play a pivotal role in modulating innate immune responses to affect the clinic outcomes in patients under systemic inflammation.

In this study, we showed that plasma Prdx1 increased immediately in a cohort of pediatric patients following CPB, and this elevated Prdx1 was correlated to a decrease in HLA-DR expression and the rise of plasma IL-10 production, as well as a hypo-responsiveness of macrophage to endotoxin and a higher incidence of in-hospital infection. We also presented evidences that cell surface engagement of TLR4 and subsequent clathrin-dependent endocytosis was essential for Prdx1 to trigger IL-10 induced endotoxin tolerance in phagocytes. Correspondingly, inhibition of Prdx1 internalization in phagocytes could reverse the hypo-responsiveness in response to LPS and targeting endocytosis of Prdx1 may be a promising therapeutic approach to minimize the occurrence and severity of CPB-induced immunoparalysis.

2. Materials and methods

2.1. CPB patient selection

A cohort of pediatric patients less than 3 years of age undergoing congenital cardiac surgery involving CPB were enrolled at National Taiwan University Hospital. Patients were excluded if they had active infection or inflammation preoperatively, were neonates with gestational ages less than 36 weeks, or weighed less than 2500 g. This study protocol was approved by the local research ethics committee (Internal Review Board number 201807127RIND), and informed consents were obtained from parents of the recruited patients.

2.2. Outcome definitions

Demographic, clinical, and culture data were obtained from electronic medical records. If postoperative infection was suspected in the setting of SIRS within 30 days after the surgery, blood, urine, or sputum samples were sent to the laboratory for culture, and patients were classified as "infected" if any final culture report was positive.

2.3. Blood sampling

Blood samples (3.0 mL) were drawn from arterial or central venous lines at the following time points: immediately after insertion of a central venous catheter during anesthetic induction, at the end of CPB, and at day 1, day 3 after CPB. The withdrawn blood would be collected into lithium (LH) heparin containing tubes for *ex vivo* lipopolysaccharide (LPS) stimulation experiment, or into ethylenediamine tetraacetic acid (EDTA) containing tubes, centrifuged at $2000 \times g$ for 15 min at 4 °C to collect plasma, which was aliquoted and stored at −80 °C for later analysis. After centrifugation, the cell pellets were diluted with PBS and gently layered over an equal volume of Ficoll (Invitrogen, Carlsbad, CA. USA) in a tube to isolate peripheral blood mononuclear cells (PBMCs). After washing with phosphate-buffered saline (PBS), 20 μL of RNAlater stabilization solution (Invitrogen) was added to the collected PBMCs and stored at −80 °C for RNA extractions.

2.4. Flow cytometric analysis

HLA-DR expressions on monocytes were investigated by adding 100 μL of EDTA anticoagulated whole blood to the combination of the following mouse anti-human antibodies (BD Biosciences, San Jose, CA. USA): 10 μL of phycoerythrin (PE) conjugated anti-CD14 and 10 μL of peridinin-chlorophyll-protein conjugated anti-HLA-DR. Cells were also labeled with negative isotype control antibodies. After incubation for 20 min at room temperature in the dark, red blood cells were lysed by 1.5 mL of BD lysing buffer, and white blood cells were washed twice with 1.5 mL of PBS containing 1 % fetal bovine serum (FBS, Invitrogen) and 0.1 % sodium azide (washing buffer). After centrifugation, the cells were fixed in 0.5 mL of PBS with 0.25 % paraformaldehyde (fixation buffer) and kept on 4 °C until analysis. For CD14 and TLR4 expression on monocyte, 100 μL of PBMCs (5×10^5 cells) from a healthy volunteer were added to a combination of 10 μL of PE conjugated anti-CD14 and 12 μL of biotinylated anti-TLR4 antibodies. After incubation for 2 h at 4 °C, the cells were washed and further incubated with 5 μL of allophycocyanin conjugated streptavidin for another 1 h before wash and fixation. For each test, a minimum of 20,000 leukocytes were acquired on BD Calibur flow cytometer and analyzed with CellQuest software. Monocytes were gated in a side scatter (SSC)/CD14$^+$ dot plot, HLA-DR positive monocytes and TLR4 and CD14 expressions were gated using isotype controls within CD14$^+$ monocytes.

To examine the interaction of Prdx1 with TLR2/TLR4, the human PBMCs or mouse RAW264.7 macrophages (5×10^5 cells) were incubated with 10 μg/mL mouse anti-TLR2 monoclonal antibody (mAb), mouse anti-TLR4 mAb, and isotype-matched antibody (all from Invitrogen) for 60 min at 37 °C followed by incubation with fluorescein isothiocyanate (FITC)-conjugated recombinant Prdx1 (FITC-Prdx1) for another 30 min at 4 or 37 °C. Cells were washed and re-suspended in fixation buffer, and Prdx1 specific fluorescence was measured by flow cytometry using CellQuest data acquisition and analysis software as described above.

2.5. Ex vivo cytokine production

The capacity of leukocyte to produce inflammatory cytokines was examined by challenging whole blood from the patients with LPS *ex vivo*. The RPMI 1640 culture medium only or culture medium supplemented with 12.5 ng/mL LPS, was stored at −80 °C and brought to room temperature before use. LH anticoagulated whole blood (0.2 mL) drawn from the patients at various time points was added to 0.8 mL of the culture medium with or without LPS, incubated at 37 °C in a humidified incubator maintaining 5 % CO_2 for 4 h, and then the cultures were centrifuged at $1600 \times g$ and the supernatants were stored at −80 °C until cytokine analysis by ELISA. In non-stimulated samples, the measurements of TNF-α production all fell below the detection limit.

2.6. RNA extraction and qRT-PCR analyses

Total RNA of PBMCs and cell lines were extracted and purified using the PureLink™ RNA mini kit according to the manufacturer's instructions (Invitrogen). The mRNA expressions in cells were evaluated by using Kapa SYBR Fast One-Step quantitative reverse transcription-polymerase chain reaction (qRT-PCR) kit (Kapa Biosystem, Wilmington, MA. USA). Briefly, 20 ng of the purified RNA was transcribed into

cDNA, which was thereafter examined by qRT-PCR with gene specific primers as shown in Table 1. The forward primers were designed to cover an exon-exon junction to prevent amplification of genomic DNA. The amplification of these sequences and the probes with the production of copies of target mRNA were specifically identified during the PCR analysis on a CFXconnect Real-Time PCR Detection System (Bio-Rad, Hercules, CA, USA). A primer pair for the detection of human glyceraldehyde-3-phosphate dehydrogenase (GAPDH) was used as the internal control for RNA isolated from THP-1-derived macrophages. For RNA obtained from PBMCs of the patients, peptidylpropylisomerase B (PPIB) was used as reference gene for HLA-DR alfa chain (HLA-DRA) [13,25]. A specific amount of RNA isolated from THP-1 cells was used on each plate as a calibrator [CV% of 0.48 % (PPIB), 0.5 % (HLA-DRA) between plates], and gene expression levels are expressed as fold change relative to the calibrating sample using the formula $2^{\Delta Ct}$.

2.7. Cloning, mutagenesis, expression, and purification of human recombinant Prdx1 protein

The entire coding region of human Prdx1 was amplified from human cDNA by PCR using specific primers as follows: forward: 5′-CGCGGATCCGTCTTCAGGAAATGCTAAA-3′ and reverse: 5′-CCCAAGCTTACTTCTGCTTGGAGAA-3′, containing a BamHI and a HindIII restriction site respectively. The purified PCR product was cleaved using endonucleases BamHI and HindIII (New England Biolab, Ipswich, MA, USA) and was ligated into the pET15b vector to construct a plasmid (Prdx1/pET15b) expressing histidine-tag (His-tag) recombinant Prdx1 protein. Using the Prdx1/pET15b as a template, site-directed mutagenesis of Cys^{83} to Ser^{83} was performed to generate point mutated Prdx1 (rPrdx1C83S) by PCR with the following primers: forward: 5′-GGATTCTCACTTCTCTCATCTAGCATGGGTC-3′ and reverse: 5′-GACCCATGCTAGATGAGAGAAGTGAGAATCC-3′. The wild type and mutated Prdx1 constructs were verified by DNA sequencing. The recombinant plasmids were transformed into *Escherichia coli* BL21 (DE3) strain. After the expression of the recombinant protein was confirmed, the bacteria were centrifuged and the pellet was re-suspended in 50 mM Tris-HCl lysis buffer containing 500 mM NaCl and 40 mM imidazole (pH7.5). The bacterial lysate was sonicated on ice, centrifuged again at $3000 \times g$ for 10 min at 4 °C. The supernatant was collected and the His-tag fusion protein was purified by Ni$^+$ Sepharose (GE Healthy Care Life Science, Buckinghamshire, UK) and desalted using Amicon ultracentrifugal filter units. Endotoxin contamination was removed by incubating the protein with endotoxin removal resin (Thermo Fisher Scientific, Carlsbad, CA. USA) for 2 h at 4 °C. The purified proteins were tested for endotoxin level using a limulus amebocyte lysate assay (Genscript USA Inc, Piscataway, NJ, USA). The concentrations of purified proteins were measured using a Bicinchoninic Acid (BCA) protein assay kit (Thermo Fisher Scientific).

2.8. FITC labeling of recombinant Prdx1

FITC-Prdx1 was prepared by incubating the purified rPrdx1 with FITC using a commercially available FITC antibody labeling kit from Pierce following the manufacturer's protocol. Protein amounts were quantified using a standard Lowry assay. The F:P (fluorescence:protein) ratio was calculated according to the manufacturer's instructions using the optical density at 495 nm (FITC absorbance) and 280 nm (protein absorbance).

2.9. Cell culture treatment

The human monocytic THP-1 and mouse macrophage (RAW264.7) cell lines were maintained in RPMI 1640 and DMEM medium respectively (both were supplemented with 10 % heat-inactivated FBS, 100 unit/mL penicillin, and 100 μg/mL streptomycin, all from Invitrogen) at 37 °C in a humidified incubator maintaining 5 % CO$_2$. Macrophages derived from THP-1 cell line were obtained by treating cells with 20 ng/mL phorbol 12-myristate 13-acetate (Sigma-Aldrich, St. Louis, MO. USA) for 24 h and followed by resting for 3–5 days with RPMI 1640 culture medium. Human PBMCs from healthy volunteers were obtained as described earlier [24]. The recombinant wild type and mutated Prdx1, IL-10 (PeproTech, Rocky Hill, NJ. USA), patients' plasma, LPS (*Escherichia coli* serotype 0111:B4, Sigma-Aldrich), and dynasore (Sigma-Aldrich) were added to the corresponding cells as indicated in the figures before cells or culture medium were harvested and analyzed.

2.10. ELISA for Prdx1 and cytokine analysis

Plasma Prdx1 levels were measured by an ELISA kit from Northwest Life Science Specialties (Vancouver, WA, USA). Cytokine levels in plasma or cell culture supernatant were determined separately using ELISA kits for TNF-α, IL-6, and IL-10 (BD Biosciences).

2.11. Pull down assay

Mouse RAW264.7 macrophages were incubated with His-tagged rPrdx1 (10 μg/mL) or not at 37 °C for 1 h, after washing twice with cold PBS and lysed with CSK buffer, the cell lysates were incubated with 25 μL of Ni$^+$ Sepharose beads at 4 °C overnight. After washing, captured proteins on the beads were separated by sodium dodecyl sulphate–polyacrylamide gel electrophoresis (SDS-PAGE) and analyzed by Western blot using antibodies recognizing TLR2 (Cell Signaling Technonogy, Danvers, MA. USA), TLR4 (Santa Cruz Biotechnology, Dallas, TX. USA), or 6 × His-tag (Sigma-Aldrich).

2.12. Transfection, and immunoprecipitation

RAW264.7 cells were transfected with FLAG-tagged human TLR2 or TLR4 expression DNA constructs (gifts from Dr. Li-Chung Hsu, Institute of Molecular Medicine, National Taiwan University College of Medicine) using PolyJet transfection reagent (SignaGen laboratories, Frederick, MD. USA) and opti-medium (Invitrogen) according to the manufacturer's protocol. The tranfected cells were harvested with CSK buffer 3 days after the transfection, and the cell lysates were immunoprecipitated with 4 μg of mouse anti-FLAG M2 antibody (Sigma-Aldrich) overnight at 4 °C. Then, 25 μL of Protein G-agarose beads (GE Healthy Care Life Science) were added to the lysates and incubated for another 4 h. The beads were washed with lysis buffer and subjected to SDS-PAGE for

Table 1
The sequence of primers used for quantitative reverse transcription-polymerase chain reaction.

Genes	Forward (5′-3′)	Reverse (5′-3′)	size (bp)
PPIB	ACAGGAGAGAAAGGATTTGGCT	AAGTTCTCATCGGGGAAGCG	143
GAPDH	GTTCGTCATGGGTGTGAACCA	GTCTTCTGGGTGGCAGTGATG	171
TNF-α	GCTGCACTTTGGAGTGATCG	TATCTCTCAGCTCCACGCCA	215
HLA-DRA	GGGCTATCAAAGAAGAACATGTGA	GCCTCAAAGCTGGCAAATCG	172

The sequences of primers used for each gene and sizes of PCR products are shown.
PPIB, peptidylpropylisomerase B; GAPDH, glyceraldehyde-3-phosphate dehydrogenase; TNF, tumor necrosis factor; HLA-DRA, human leukocyte antigen-DR alpha chain.

Western blot analysis using polyclonal rabbit anti-human Prdx1 antibody (Abcam, Cambridge, MA, USA).

2.13. Western blotting

The protein samples were applied to 10–15 % acrylamide SDS gels and transferred to nitrocellulose membranes (Merck Millipore, Darmstadt, Germany) by electroblotting. After blocking in 5 % non-fat milk in PBS containing 0.05 % Tween 20, membranes were probed with various primary antibodies: polyclonal rabbit anti-human Prdx1 antibody (Abcam), mouse anti-His (Sigma-Aldrich), followed by detection with anti-rabbit-IgG-horse-radish peroxidase conjugate (Sigma-Aldrich) or anti-mouse IgG horseradish peroxidase conjugate (Stratagene, Agilent Technologies, Santa Clara, CA. USA). Western blots were developed using advanced chemiluminescence (ECL) reagents (GE Healthcare, Amersham, UK) and exposed to autoradiography using Hyper-film (GE Healthcare).

2.14. Statistical analysis

Medians and interquartile ranges were presented in some figures due to non-normal distribution characteristic of most data. Continuous data were also expressed as mean $\pm$ standard deviation (SD) in figures when appropriate. Categorical variables were compared using X^2 or Fisher's exact test. The significant differences between groups were compared by Mann–Whitney U test or Student's t-test. The correlated data were analyzed by the Spearman's test for simple correlation, or determined using Bland and Altman analysis for repeated measures correlation [26]. All tests are two-sided, and $P < 0.05$ is considered significant. The data were analyzed using SPSS 17.0 (SPSS Inc, Chicago, IL. USA).

3. Results

3.1. Patient characteristics

Fourty patients were enrolled with a median age of 5.5 months (range 2.25–13.25 months), median weight of 6.4 kg (range 4.3–8.5 kg), median duration of ICU stay of 6 days (range 3–26.5 days), median duration of hospital stay of 18 days (range 10–42.5 days) and an overall mortality of 7.5 %. The median duration of CPB for all patients was 87 min (range 68–151 min). Eleven (27.5 %) patients who fulfilled the criteria indicative of CPB associated SIRS were identified during the first six days of the postoperative period, and 8 of them were documented to have positive microbial culture results within 30 days after surgery. The baseline characteristics of these patients were depicted in Table 2.

Table 2
Characteristics of patients with and without postoperative infection.

Parameter	no Infection (n = 32)	Infection (n = 8)	P value
Age (months)	6 (4.0–13.3)	2.5 (0.5–16)	0.176
Male, n (%)	24 (75.0)	7 (87.5)	0.655
Weight (kg)	7.07 (5.80–8.79)	3.85 (3.29–6.58)	0.023
CPB time (minutes)	80 (67–113)	166 (107–233)	0.001
Neonates, n (%)	4 (12.5)	2 (25.0)	0.58
Aortic clamp time (minutes)	44 (32–58)	97 (45–127)	0.023
Duration of ICU stay (days)	5 (2.3–8.8)	107.5 (28–159)	<0.001
Duration of hospital stay (days)	14 (10–20.8)	161 (34–184)	<0.001
Mortality prior to hospital discharge, n (%)	0 (0.0)	1 (12.5)	0.275

Continuous data values are shown as medians with inter-quartile ranges. The number of patients with frequency (%) is shown for categorical data. The listed P values of statistical tests were calculated using Mann–Whitney U for continuous data and the X^2 or Fisher's exact test for categorical data.
CPB, cardiopulmonary bypass; ICU, intensive care unit.

Longer duration of CPB and aortic clamping, and smaller body weight were significant risk factors for postoperative infection following CPB. Although previous studies have identified age as a contributing factor for nosocomial infection after cardiac operation [27–29], our analysis did not show a similar result. We reasoned this discrepancy could be due to a small sample size in the infected group.

Infected patients had higher levels of plasma Prdx1, IL-6, and IL-10 after CPB than non-infected patients.

To decipher the role of DAMP molecule Prdx1 in the recovery process after CPB, the dynamic changes of plasma Prdx1 and inflammatory cytokines in the infected and non-infected patients were monitored during the peri-operative period (Fig. 1). Plasma Prdx1 rose immediately after CPB and remained significantly elevated at day 1 and day 3 in the infected patients compared to the non-infected patients (Fig. 1A). Similar difference was also noted for plasma IL-6 levels in the infected patients verse the non-infected patients after CPB (Fig. 1B). The anti-inflammatory cytokine IL-10 increased immediately after CPB in these patients, and the IL-10 fell thereafter in non-infected group with IL-10 remaining significantly higher in the infected group at day 1 and day 3 (Fig. 1C). In contrast to IL-10 and IL-6, pro-inflammatory cytokine TNF-α did not change too drastically throughout the whole observational period, and the TNF-α levels were not significantly different between both groups of patients possibly reflecting a generally immunosuppressive status of subjects receiving CPB (Fig. 1D) [13].

Immunosuppression is more profound in infected patients than non-infected patients.

Given these pediatric patients were aseptic before operation but some of them suffered from infection after CPB, we reasoned that CPB incurred an immunosuppessive influence during the cardiac operative procedure and then led to subsequent in-hospital infection in the more severely immunosuppressed patients. To test this hypothesis, the capacity of leukocytes responding to LPS challenge was examined by a pilot study in a selected group of patients whose clinical characteristics were shown in supplemental table 1. The ex vivo productions of inflammatory mediator TNF-α in all patients were severely impaired immediately at CPB wean off. However, the repressed cytokine productions recovered shortly at day 1 and day 3 after the surgery, reaching the level noted at pre-CPB time (Fig. 2A). In the same group of patients, HLA-DR expressions on monocyte decreased after CPB, with the lowest expression being observed at day 1 (Fig. 2B). HLA-DRA mRNA level has been reported to correlate well with flow cytometric analysis of membrane HLA-DR [30]; therefore, HLA-DRA gene expressions were also analyzed in PBMCs of the main cohort (the patients whose clinical outcomes, including infection history, had been well recorded, Table 2). Indeed, HLA-DRA expressions were significantly lower in infected patients as early as CPB wean-off than those who did not develop infection (Fig. 2C). Moreover, to verify whether humoral inflammatory mediators in plasma is crucial in determining the immune suppression, secretion of TNF-α by THP-1 macrophages stimulated with LPS (4 h) was measured in the presence of patient's plasma (1 h prior to addition of LPS) obtained from all time points. Similar to the earlier result shown in a smaller group of patients (Fig. 2A), ex vivo TNF-α response was repressed by the patients' plasma obtained at the end of CPB as compared to the plasma retrieved before CPB (Fig. 2D). Furthermore, this suppressive effect was more profound for plasma from the infected patients compared to those from non-infected patients.

Secretion of Prdx1 after CPB is involved in the production of IL-10 and development of immunoparalysis.

Plasma Prdx1 levels at the moment of CPB wean-off were positively correlated with duration of CPB procedure ($r = 0.418$, $P = 0.007$, Fig. 3A). During the observational period, the peak level of plasma Prdx1 correlated well with the lowest mRNA expression of HLA-DRA ($r = -0.415$, $P = 0.008$, Fig. 3B). Plasma Prdx1 levels were also positively correlated with IL-10 levels at all the 4 time points when the samples were collected ($r = 0.606$, $P < 0.001$, Fig. 3C). Notably, the extents of these plasma to suppress THP-1 macrophages immune responsiveness,
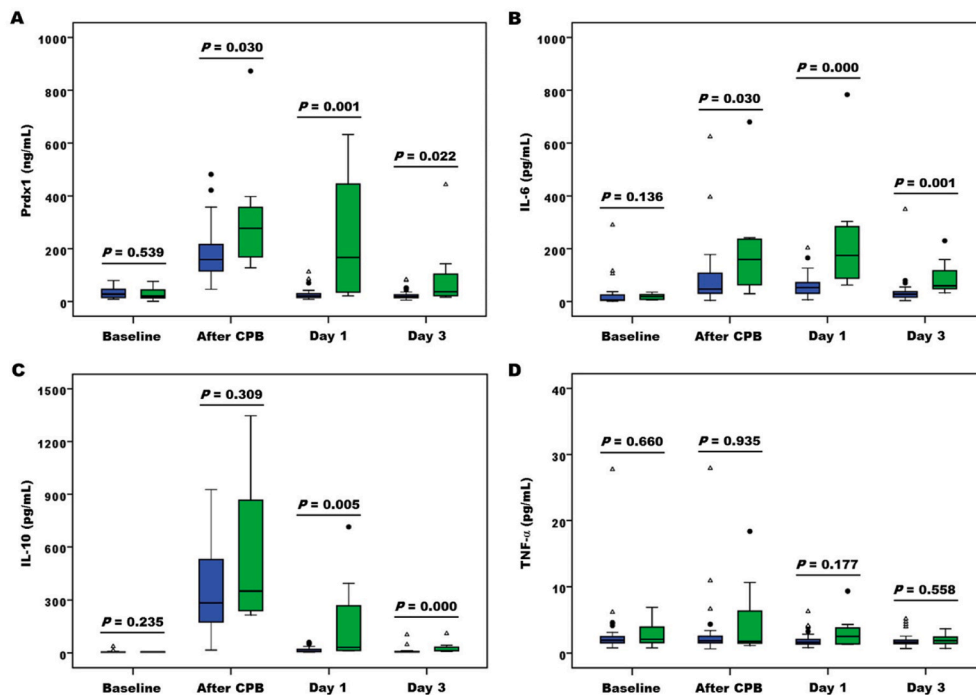
Fig. 1. Higher Prdx1 and inflammatory cytokine levels precede the occurrence of septic infection after cardiopulmonary bypass. Plasma peroxiredoxin 1 (Prdx1) (**A**), interleukin 6 (IL-6) (**B**), IL-10 (**C**) and tumor necrosis factor (TNF-α) (**D**) levels in pediatric patients at pre-operation, the end of CPB, 1 day, and 3 days after cardiac surgery were assayed in infected (n = 8, *green boxes*) and non-infected (n = 32, *blue boxes*) patients. Data were expressed as median and interquartile range; *solid circle* and *open triangle* indicated mild and extreme outliers respectively. Statistical differences between groups were analyzed by Mann–Whitney *U* test. (For interpretation of the references to colour in this figure legend, the reader is referred to the Web version of this article.)
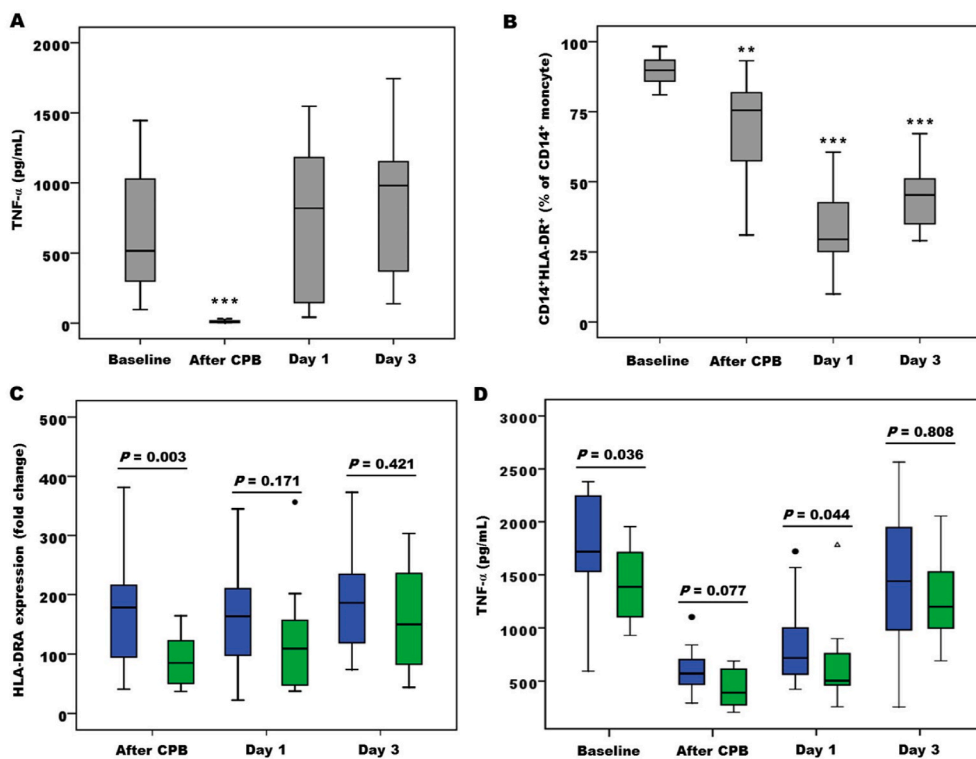

Fig. 2. Blood leukocytes and plasma from infected patients show more suppressive immune responses and effects than that in non-infected patients. TNF-α production in whole-blood after LPS stimulation for 4 h (**A**) and percentage of HLA-DR$^+$ cells in CD14$^+$ monocytes (**B**) were analyzed in a selected group of patients (n = 16) at the indicated time points during the perioperative period, **$P < 0.01$, ***$P < 0.001$ as compared to baseline. (**C**) HLA-DRA gene expressions in PBMCs were assayed by qRT-PCR in infected (n = 8, *green boxes*) and non-infected (n = 32, *blue boxes*) patients at the indicated time points following CPB. (**D**) Plasma obtained from infected (n = 8, *green boxes*) and non-infected (n = 28, *blue boxes*) patients at the indicated time points were added to THP-1 macrophages (5 × diluted in the culture medium) 1 h prior to stimulation with LPS for 4 h, and TNF-α productions in the supernatants were analyzed by ELISA. Data represented median and interquartile range; *solid circle* and *open triangle* indicated mild and extreme outliers respectively. Statistical differences between groups were analyzed by Mann–Whitney *U* test. (For interpretation of the references to colour in this figure legend, the reader is referred to the Web version of this article.)

as measured by the TNF-α production in response to LPS challenge, were negatively correlated to the IL-10 levels present in the corresponding plasma. ($r = -0.470$, $P < 0.001$, Fig. 3D). This finding implied that the plasma Prdx1 was possibly through IL-10 induction to elicit its immunosuppressive effect.

3.2. Induction of IL-10 secretion and LPS tolerance is dependent upon Prdx1 structure

Human Prdx1 can induce TLR4-dependent pro-inflammatory TNF-α and IL-6 secretions from macrophages, and this effect is likely dependent on its structure and chaperon activity [19]. However, the capacity and biochemical determinant of Prdx1 to induce anti-inflammatory IL-10 production has not been investigated. Given the above results that the
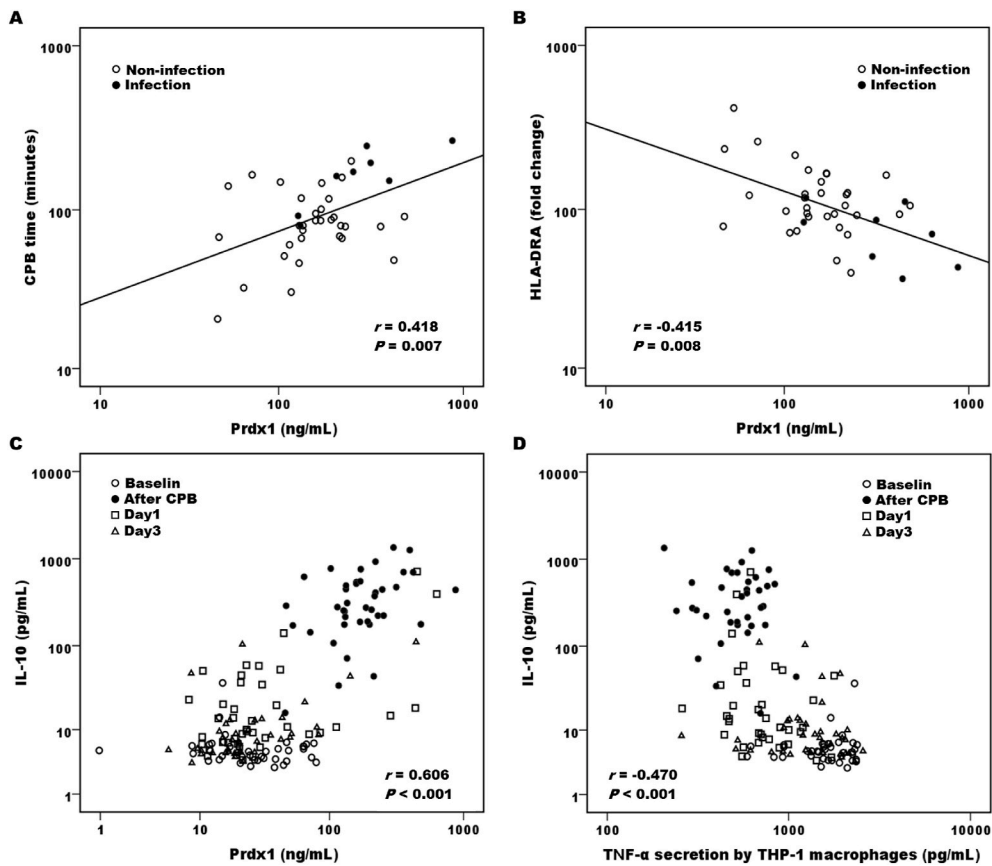
Fig. 3. Increased Prdx1 levels are associated with longer CPB duration, less MHC class II expression, and higher IL-10 production that is correlated with a status of immunosuppression. Correlation between (**A**) CPB times and plasma levels of Prdx1 at the end of CPB, (**B**) peak levels of plasma Prdx1 and the lowest expression of HLA-DRA mRNA in PBMCs from patients right after CPB, (**C**) plasma Prdx1 and IL-10 levels (n = 40, 4 time points per patient), and (**D**) plasma levels of IL-10 and TNF-α production by LPS-stimulated THP-1 macrophages in the presence of plasma obtained from patients (n = 36, 4 time points per patient). Spearman correlation (**A**, **B**) or Bland and Altman method (**C**, **D**) were used to calculate the correlation coefficients and statistical differences.

plasma Prdx1 levels in patients were negatively correlated to the innate immunity activation marker HLA-DRA (Fig. 3B) and positively correlated to IL-10 (Fig. 3C), we thus hypothesized that Prdx1 could induce IL-10 production and trigger subsequent immunosuppression in phagocytes. To determine whether the ability of Prdx1 in cytokine production was related to its structure, wild type and rPrdx1C83S mutant were examined in parallel. To eliminate endotoxin contamination during the preparation of the recombinant Prdx1, these proteins were treated with endotoxin removal resin, and the purified rPrdx1 and rPrdx1C83S proteins were noted to contain a negligible level of endotoxin (0.035 ± 0.006 EU/ml and 0.046 ± 0.015 EU/ml respectively). We observed that unlike wild type rPrdx1 which existed as a decamer, mutation of cysteine Cys83 in Prdx1 prevented its high molecular weight formation and existed mainly as a dimer as previously reported (Fig. 4A) [31]. Having demonstrated the importance of intermolecular and intramolecular disulfide bonds in the biochemical property of Prdx1, we conjugated fluorescein to purified recombinant Prdx1 (FITC-Prdx1) and used it as a probe in the absence or presence of dithiothreitol (DTT) to trace the fate of Prdx1 following its contact with phagocytes. Indeed, Prdx1 binding and subsequent internalization to macrophages depended upon the presence of high molecular forms as binding at 4 °C and endocytosis at 37 °C of Prdx1 were both significantly decreased with DTT pretreatment which denatured rPrdx1 to its monomeric form by reducing the intermolecular and intramolecular disulfide bonds (Fig. 4B). Moreover, the rPrdx1 could induce IL-10 production comparable to the extent as elicited by LPS (Fig. 4C), whereas, both the pro-inflammatory and anti-inflammatory cytokines-inducing abilities of rPrdx1 were diminished when rPrdx1 was pretreated with reducing agent DTT (Fig. 4C and D). There was a significant reduction of TNF-α and IL-10 release from macrophages stimulated with rPrdx1C83S (Fig. 4E and F). Taken together, the presence of key cysteine residues to preserve the higher molecular weight forms in Prdx1 can be a

prerequisite for its cytokine-inducing activity via binding and subsequent internalization to macrophages.

To examine the potential of Prdx1 as an inducer of immunoparalysis, human THP-1 macrophages were primed with LPS, recombinant Prdx1 (rPrdx1), or Prdx1C83S (rPrdx1C83S) for 24 h prior to LPS stimulation and TNF-α production was determined. Lipopolysaccharide and rPrdx1 pretreatments significantly attenuated both the TNF-α protein release and mRNA expression in response to LPS stimulation (Fig. 4G), while pretreatment of these cells with rPrdx1C83S only led to a marginal reduction of TNF-α production in response to LPS challenge. Moreover, treatment of rPrdx1 with heating significantly abrogated its induction of LPS tolerance in RAW264.7 macrophages, while heating did not block this effect of LPS (Fig. 4H), indicating the observed immune tolerance is specific to rPrdx1 instead of any contaminated endotoxin left from the purification step of this recombinant protein.

We also explored the impact of IL-10 signaling on Prdx1-induced LPS tolerance in human phagocytes, and it was noted that recombinant IL-10 pretreatment inhibited TNF-α secretion from THP-1 macrophages to the extent as observed in LPS or rPrdx1-mediated immune tolerance (Fig. 4I). In contrast, the presence of IL-10 receptor antibody during pre-incubation period of rPrdx1 significantly diminished the immune tolerance effect of rPrdx1 and reverted the response of human PBMCs to subsequent LPS challenge (Fig. 4J). Intriguingly, there was no apparent effect of IL-10 receptor blocking on the LPS induced immune hyporesponsiveness (Fig. 4J). This implied that there existed an IL-10 independent pathway to mediate the endotoxin induced immune tolerance.

Clathrin-dependent endocytosis of Prdx1/TLR4 is required for Prdx1-mediated LPS tolerance.

Like many other DAMPs, Prdx1 is shown to interact with both the TLR2 and TLR4 receptors [20]. Although our pull-down assay demonstrated that only TLR4 but not TLR2 interacted with his-tagged Prdx1 (Fig. 5A), co-immunoprecipitation analysis showed that both the
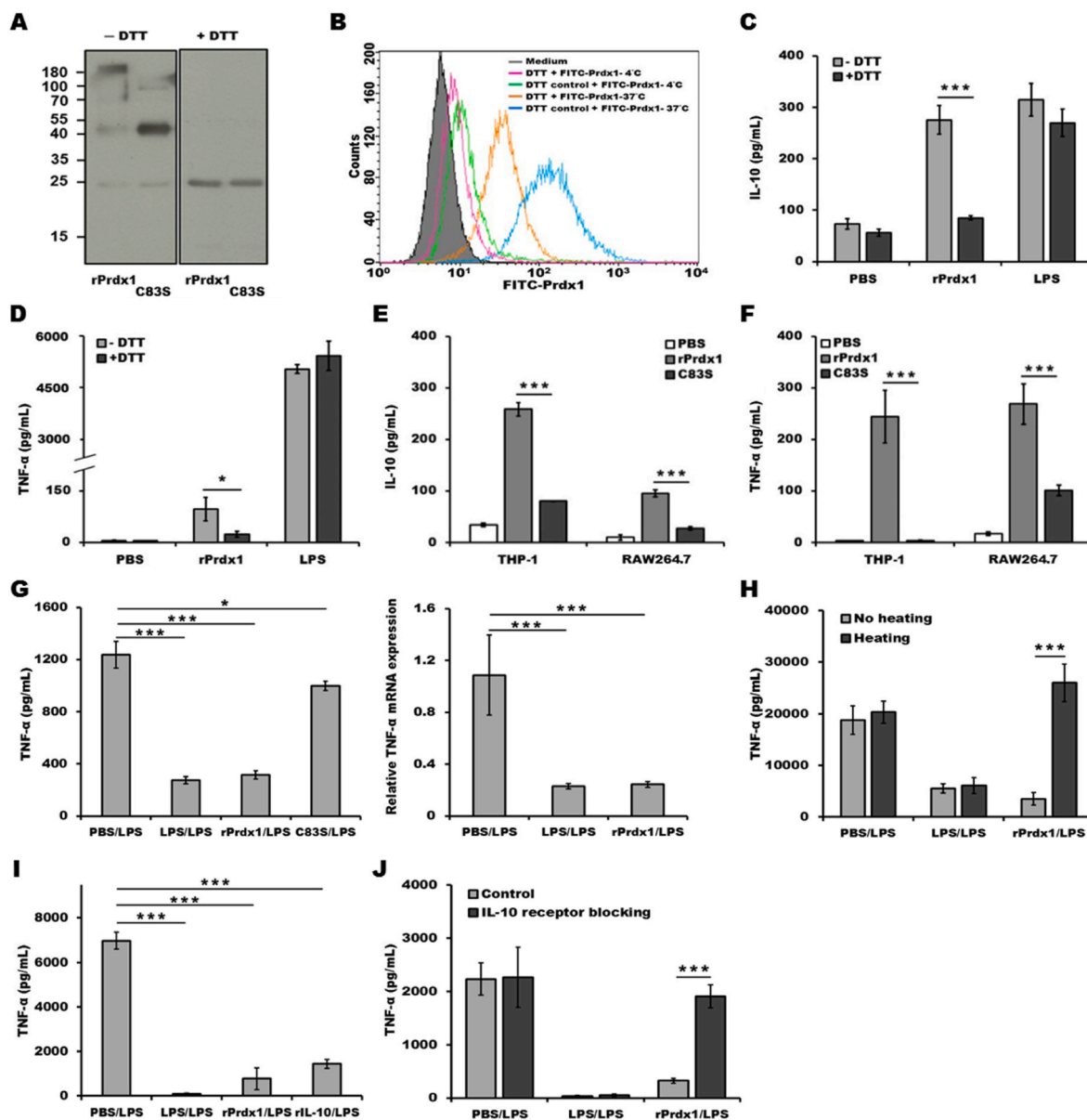
Fig. 4. Prdx1 induces IL-10 production and IL-10-dependent LPS tolerance in phagocytes. (A) Immunoblot analysis using mouse anti-His tag antibody of his-tagged human Prdx1 (rPrdx1) and rPrdx1C83S (C83S) recombinant proteins separated by SDS-PAGE under non-reducing (-DTT) and reducing (+DTT) conditions. Molecular weight markers in kilodaltons were denoted on the left. **(B)** FITC-labeled rPrdx1 was pretreated with DTT (10 mM) at room temperature for 1 h and then added to mouse RAW264.7 macrophages at 4 or 37 °C for 30 min. Separate assays were conducted using FITC-Prdx1 which had not been pretreated with DTT, but with the same amount of DTT being added directly to the incubation medium as DTT controls. The fluorescence of these cells was measured by flow cytometry. Human THP-1 macrophages were stimulated with DTT pretreated (10 mM for 1 h) or non-treated PBS, rPrdx1, or LPS for 24 h before IL-10 **(C)** or TNF-α **(D)** level in culture medium was analyzed by ELISA. Human THP-1 and mouse RAW264.7 macrophages were incubated with PBS, rPrdx1 (10 μg/mL) or rPrdx1C83S (10 μg/mL) for 24 h, and the culture supernatants were analyzed for IL-10 **(E)** and TNF-α **(F)** by ELISA. **(G)** THP-1 macrophages were incubated with PBS, LPS (10 ng/mL), rPrdx1 (10 μg/mL), or rPrdx1C83S (10 μg/mL) for 24 h and all four different groups of cells were subsequently re-challenged with LPS (10 ng/mL) for another 4 h, TNF-α secretion in culture medium and mRNA expression in cells were analyzed by ELISA (left) and qRT-PCR (right) respectively. **(H)** PBS, LPS (10 ng/mL), or rPrdx1 (10 μg/mL), that were either pretreated with heating (100 °C for 10 min) or not, was added to RAW264.7 macrophages for 24 h before being re-challenged with LPS (10 ng/mL) for 4 h, and the TNF-α levels in the supernatant were analyzed by ELISA. **(I)** THP-1 macrophages were pretreated with PBS, LPS (10 ng/mL), rPrdx1 (10 μg/mL), or recombinant IL-10 (rIL-10, 10 ng/mL) for 24 h and the cells were challenged with LPS (10 ng/mL) for 4 h. TNF-α secretion in culture medium was analyzed by ELISA. **(J)** Human PBMCs were incubated with PBS, LPS, or rPrdx1 in the presence or absence of an IL-10 receptor blocking antibody (50 μg/mL) for 24 h. Then, cells were stimulated with LPS (10 ng/mL) for 4 h and TNF-α secretion in the culture supernatants was analyzed. Data represented means of triplicate samples; error bars represented standard deviations (SDs). *$P < 0.05$, and ***$P < 0.001$.

over-expressed FLAG-tagged human TLR2 and TLR4 could bind to endogenous Prdx1 in RAW264.7 macrophages (Fig. 5B). Compared to TLR2, less TLR4 was isolated by the anti-FLAG immunoprecipitating antibody presumably reflecting the different expression efficiencies of the two plasmids used in the transient transfection. Notably, although less TLR4 was immunoprecipitated, similar levels of Prdx1 were isolated

in the corresponding immune complex implying that the binding affinity of TLR4 for Prdx1 should be stronger than that of TLR2. Given these findings from our pull-down and co-immunoprecipitation assay which established a physical interaction between Prdx1 and TLR4, we then focused to interrogate the consequences of this molecular interaction at cellular level. To this end, we used the fluorescein conjugated Prdx1
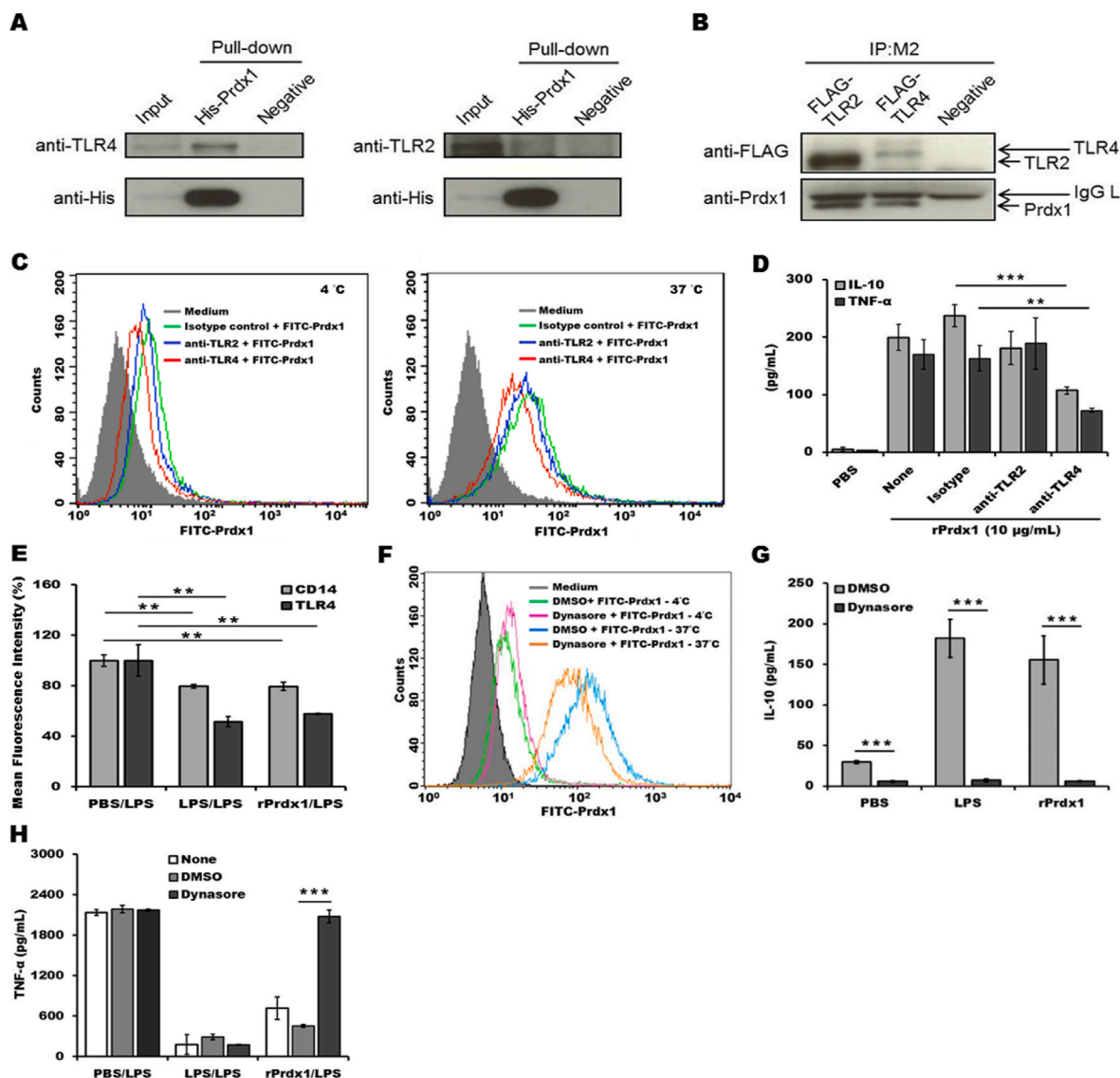
Fig. 5. Endocytosis of Prdx1/TLR4 complex plays a crucial role in Prdx1-induced IL-10 secretion and the development of LPS tolerance. (**A**) Mouse RAW264.7 macrophages were incubated with His-tagged rPrdx1 or not for 1 h, and the cell lysates were incubated with Ni^+ Sepharose beads. After washing, captured proteins on the beads were processed by SDS-PAGE and subjected to Western blot analysis using antibodies recognizing TLR2, TLR4, or $6 \times$ His-tag. (**B**) RAW264.7 macrophages were transfected with FLAG-tagged TLR2 or TLR4 expressing DNA constructs and cell lysates were immunoprecipitated with mouse anti-FLAG antibody. The precipitates were further subject to SDS-PAGE followed by Western blot analysis for the presence of Prdx1. Blots were also probed with antibody to FLAG as a loading control. (**C**) Human PBMCs were pretreated with neutralizing mAb to either TLR2, TLR4, or isotype-matched control antibody (10 μg/mL) at 37 °C for 1 h and further incubated with FITC-labeled rPrdx1 (10 μg/mL) for 30 min at 4 or 37 °C, the cell-bound fluorescence was detected by flow cytometry. (**D**) Human PBMCs were pretreated with neutralizing mAb to either TLR2, TLR4, or isotype-matched control antibody at 37 °C for 1 h and further incubated with rPrdx1 (10 μg/mL). After 24 h, TNF-α and IL-10 cytokine levels in culture supernatants were measured by ELISA. (**E**) Human PBMCs were incubated with either PBS, LPS or rPrdx1 for 24 h, and re-challenged with LPS (10 ng/mL) for additional 4 h, cell surface expressions of CD14 and TLR4 were analyzed by flow cytometry. (**F**) RAW264.7 macrophages were pretreated with dynasore (80 μM) or DMSO at 37 °C for 1 h and further incubated with FITC-labeled rPrdx1 (10 μg/mL) at 4 or 37 °C for 30 min. The fluorescence was measured by flow cytometry. (**G**) THP-1 macrophages were treated with dynasore (80 μM) or DMSO at 37 °C for 1 h prior to stimulation with LPS or rPrdx1 for 24 h. IL-10 levels in culture supernatants were analyzed by ELISA. (**H**) THP-1 macrophages were left untreated (none), treated with DMSO, or dynasore (80 μM) at 37 °C for 1 h prior to be incubated with PBS, LPS, or rPrdx1 for 24 h. Then, these cells were re-challenged with LPS (10 ng/mL) for 4 h and TNF-α secretion was measured by ELISA. Data represented means of triplicate samples; error bars represented SDs. **$P < 0.01$, and ***$P < 0.001$.

(FITC-Prdx1) as a surrogate marker to study the fate of Prdx1 following its contact with phagocytes. We found that both the cell surface-bound (Fig. 5C, left panel) and the endocytosed (Fig. 5C, right panel) rPrdx1-specific fluorescence intensities were lower when human PBMCs were pre-incubated with anti-TLR4 antibody than those pre-incubated with anti-TLR2 or isotype-matched control antibody. These results indicated that TLR4 was likely the main surface receptor for Prdx1. Additionally, both the pro-inflammatory TNF-α and anti-inflammatory IL-10 inducing effects of rPrdx1 were significantly reduced in human

PBMCs pre-incubated with TLR4 antibody as compared to those cells pre-treated with anti-TLR2 or isotype-matched control antibody (Fig. 5D), confirming that rPrdx1-mediated induction of IL-10 in macrophages is predominantly dependent on its interaction with TLR4. Furthermore, in vitro priming of healthy PBMCs with either LPS or rPrdx1 for 24 h led to a reduced monocytic CD14/TLR4 surface presentation as compared to unprimed controls (Fig. 5E). This observation signified the formation of a signaling endosome which has been implicated with transduction of anti-inflammatory message following LPS

engagement of TLRs at plasma membranes [32].

Clathrin-dependent endocytosis is known to be a major pathway for internalization of transmembrane receptors. Therefore, we examined whether receptor-mediated endocytosis of Prdx1 is essential for activation of IL-10. When mouse RAW264.7 macrophages were incubated with FITC-Prdx1 in the presence of dynasore, a specific dynamin inhibitor that is identified to block clathrin-dependent endocytosis, the internalization of rPrdx1 at 37 °C was impeded as reflected by the reduced fluorescence of FITC-Prdx1 in the whole cell (Fig. 5F). In contrast, RAW264.7 macrophages treated with dynasore displayed higher fluorescence intensity at 4 °C, suggesting an accumulation of rPrdx1-TLR4 complex on cell surface when the receptor-mediated endocytosis was inhibited (Fig. 5F). Concurrently, rPrdx1-mediated IL-10 induction was largely abolished in THP-1 macrophages treated with dynasore (Fig. 5G). Intriguingly, while both endotoxin and the DAMP molecule rPrdx1 could elicit significant immune hypo-responsiveness in THP-1 cells, dynasore could only relieved the immune inertia in rPrdx1, but not in LPS-pretreated cells (Fig. 5H). This discrepancy implied that LPS may employ some other mechanism to elicit immune tolerance in addition to the dynamin mediated signaling endosome formation.

4. Discussion

Our study demonstrated that Prdx1, an intracellular antioxidant fundamental for redox homeostasis, was released after CPB and, intriguingly, not only acted as a danger signal to initiate acute inflammation but also triggered destructive immunoparalysis via IL-10 induction. The findings identify Prdx1 as a crucial link between oxidative stress and immune suppression underlying postoperative infections following CPB, and unravel a promising therapeutic target for combating late complications in sterile inflammation.

The contributing factors associating CPB during cardiac surgery to SIRS include ischemia-reperfusion (I/R) injury, surgical trauma, mechanical shear stress, and contact of peripheral blood with artificial surfaces [2,3]. However, despite great advances in cardiothoracic surgery, pump and circuit design, oxygenators, and the improvement of biocompatible surfaces, a considerable inflammatory response ensues from CPB. In consequence, I/R injury has been recognized as a crucial factor contributing to aberrant inflammation during CPB [33–35]. It has been reported that prolonged CPB duration and aorta cross-clamp during cardiac surgery link to the post-operative complications [27], but the underlying mechanisms have not yet been fully elucidated. Our data showed that plasma Prdx1 increased immediately following CPB, and correlated to the CPB times, possibly reflecting the degree of hypoxic damage under I/R injury in these patients. This finding was in concurrence with our previous works in a cohort of globally ischemia patients with extracorporeal membrane oxygenation support, in whom endogenous Prdx1 was released from monocytes and tissues due to hypoxia/re-oxygenation insult [24].

It has been well documented that CPB induces immunoparalysis following pediatric cardiac surgery; Allen et al. demonstrate an association between reduced monocyte HLA-DR expression in the first 4 days following CPB and subsequent development of post-operative sepsis in children with cardiac surgery [6]. These results are reinforced in a follow-up study in which the patients with the lowest values of *ex vivo* TNF-α productions as early as day 2 following CPB are associated with progress of post-operative complications including nosocomial infection, and the reduction in TNF-α response is related to high plasma IL-10 levels in these subjects [7]. Likewise, Cornell et al. show that reduced TNF-α production capacity on post-operative day 1 predicts the development of sepsis in children undergoing CPB [8]. Apparently, our results are in agreement with these findings that immunoparalysis is associated with an increased risk for infections and consequently longer hospital stays. Our data further revealed that the increased DAMP Prdx1 was associated with an elevated level of plasma IL-10 as well as a reduced expression of monocytic HLA-DR presentation and, more importantly,

with the occurrence of postoperative infections. In addition, the results from THP-1 macrophages challenged with LPS in the presence of patients' plasma (Fig. 3D) proved that the inflammatory mediators in plasma were the major culprits for the reduced TNF-α production capacity of leukocytes.

Increased plasma levels of DAMPs are associated with the development of ensuing immunoparalysis in patients with sterile inflammation, and high circulating levels of IL-10 are implied to have a crucial role in the pathogenesis of this immunosuppression [13]. Recently, new evidences reveal that IL-10 triggers phosphorylation/activation of downstream transcription factor signal transducer and activator of transcription-3, which causes B-cell lymphoma-3 expression in MRPs-induced tolerant monocytes [14]. These results signify that the mechanisms for immunosuppression following CPB comprise downstream signaling of DAMPs and IL-10. The Prdx family proteins are known to induce pro-inflammatory cytokines like TNF-α and IL-6 through interaction with TLR4 and TLR2 [19,20,23], and this pro-inflammatory effect is independent of its peroxidase activity, but is likely dependent on its chaperon activity [19]. In this study, we confirmed that high ordered molecular formation is essential for Prdx1 binding to TLR4. It has been demonstrated that substituting Cys[83] with Ser[83] lead to striking structural and functional alterations of Prdx1 in a direction toward those characteristics of Prdx2. Compared to Prdx2, the peroxidase activity of Prdx1 is more predisposed to inactivation by H_2O_2. Coherent to this finding, the catalytic cysteine residues of Prdx1 are more susceptible to hyperoxidation than that of Prdx2 [31]. Although both the over-oxidized and reduced forms of Prdx1 exist as a decameric complex with high molecular weight, but the hyperoxidized form confers a more stable oligomer than the reduced form [36]. Therefore, this property may bestow perniciousness differentially on Prdx1 and Prdx2 based on the distinctive reactions of phagocytes in response to rPrdx1 and rPrdx1C83S.

A complex pathophysiologic interaction of innate immunity initiators, such as DAMPs and pathogen-associated molecular patterns, may be involved in the progression of multiple organ failure and mortality in patients with sterile and septic inflammation. Li et al. show that CPB during pediatric cardiac surgery inhibits the activation of TLR signal transduction pathways in monocyte with down-regulated expression of CD14, TLR4, and TLR2, thereby causing an immunosuppressive state after cardiac surgery for congenital heart disease [37]. This result is in line with our observation that monocytic CD14/TLR4 expressions were reduced on monocytes with rPrdx1 or LPS-induced endotoxin tolerance (Fig. 5E), possibly reflecting the interaction and internalization for ligand/receptor complex during activation of innate immunity. Indeed, perturbation of endocytosis by dynamin inhibitor to interfere internalization of transmembrane receptors (TLR4) blocked internalization of rPrdx1, which was essential for IL-10 production and reversed the IL-10-mediated LPS tolerance in macrophages.

In summary, our study highlighted the possible mechanisms by which Prdx1 can engender an immunoparalysis status during sterile inflammation by initiating TLR4-mediated endocytosis to induce IL-10 production in phagocytes and a profound immunosuppressive response deterring recovery from CPB-elicited SIRS after cardiac surgery. On the other hand, inhibition of Prdx1/TLR4 endocytosis to enhance a host protective pro-inflammatory response can alleviate the IL-10-mediated detrimental effects.

Declaration of competing interest

The authors declare that they have no known competing financial interests or personal relationships that could have appeared to influence the work reported in this paper.

Acknowledgements

Appendix A. Supplementary data

Supplementary data to this article can be found online at https://doi.org/10.1016/j.redox.2021.102086.

References

[1] J.M. Lord, et al., The systemic immune response to trauma: an overview of pathophysiology and treatment, Lancet (London, England) 384 (2014) 1455–1465, https://doi.org/10.1016/s0140-6736(14)60687-5.

[2] R.A. Bronicki, M. Hall, Cardiopulmonary bypass-induced inflammatory response: pathophysiology and treatment, Pediatr. Crit. Care Med. 17 (2016) S272–S278, https://doi.org/10.1097/pcc.0000000000000759.

[3] S. Wan, J.L. LeClerc, J.L. Vincent, Inflammatory response to cardiopulmonary bypass: mechanisms involved and possible therapeutic strategies, Chest 112 (1997) 676–692, https://doi.org/10.1378/chest.112.3.676.

[4] N.S. Ward, B. Casserly, A. Ayala, The compensatory anti-inflammatory response syndrome (CARS) in critically ill patients, Clin. Chest Med. 29 (2008) 617–625, https://doi.org/10.1016/j.ccm.2008.06.010, viii.

[5] W.J. Frazier, M.W. Hall, Immunoparalysis and adverse outcomes from critical illness, Pediatr. Clin. 55 (2008) 647–668, https://doi.org/10.1016/j.pcl.2008.02.009, xi.

[6] M.L. Allen, et al., Early postoperative monocyte deactivation predicts systemic inflammation and prolonged stay in pediatric cardiac intensive care, Crit. Care Med. 30 (2002) 1140–1145, https://doi.org/10.1097/00003246-200205000-00031.

[7] M.L. Allen, et al., Interleukin-10 and its role in clinical immunoparalysis following pediatric cardiac surgery, Crit. Care Med. 34 (2006) 2658–2665, https://doi.org/10.1097/01.ccm.0000240243.28129.36.

[8] T.T. Cornell, et al., Clinical implications and molecular mechanisms of immunoparalysis after cardiopulmonary bypass, J. Thorac. Cardiovasc. Surg. 143 (2012) 1160–1166, https://doi.org/10.1016/j.jtcvs.2011.09.011, e1161.

[9] A. Asea, et al., Novel signal transduction pathway utilized by extracellular HSP70: role of toll-like receptor (TLR) 2 and TLR4, J. Biol. Chem. 277 (2002) 15028–15034, https://doi.org/10.1074/jbc.M200497200.

[10] D. Rohde, et al., S100A1 is released from ischemic cardiomyocytes and signals myocardial damage via Toll-like receptor 4, EMBO Mol. Med. 6 (2014) 778–794, https://doi.org/10.15252/emmm.201303498.

[11] S. Kim, et al., Signaling of high mobility group box 1 (HMGB1) through toll-like receptor 4 in macrophages requires CD14, Mol Med 19 (2013) 88–98, https://doi.org/10.2119/molmed.2012.00306.

[12] K. Timmermans, et al., The Involvement of danger-associated molecular patterns in the development of immunoparalysis in cardiac arrest patients, Crit. Care Med. 43 (2015) 2332–2338, https://doi.org/10.1097/ccm.0000000000001204.

[13] K. Timmermans, et al., Plasma levels of danger-associated molecular patterns are associated with immune suppression in trauma patients, Intensive Care Med. 42 (2016) 551–561, https://doi.org/10.1007/s00134-015-4205-3.

[14] N. Freise, et al., Signaling mechanisms inducing hyporesponsiveness of phagocytes during systemic inflammation, Blood 134 (2019) 134–146, https://doi.org/10.1182/blood.2019000320.

[15] Z.A. Wood, E. Schroder, J. Robin Harris, L.B. Poole, Structure, mechanism and regulation of peroxiredoxins, Trends Biochem. Sci. 28 (2003) 32–40.

[16] C.H. Wilson, et al., Increased expression of peroxiredoxin 1 and identification of a novel lipid-metabolizing enzyme in the early phase of liver ischemia reperfusion injury, Proteomics 11 (2011) 4385–4396, https://doi.org/10.1002/pmic.201100053.

[17] S.G. Rhee, H.A. Woo, Multiple functions of 2-Cys peroxiredoxins, I and II, and their regulations via post-translational modifications, Free Radic. Biol. Med. 152 (2020) 107–115, https://doi.org/10.1016/j.freeradbiomed.2020.02.028.

[18] J. Bolduc, et al., Peroxiredoxins wear many hats: factors that fashion their peroxide sensing personalities, Redox Biol 42 (2021), 101959, https://doi.org/10.1016/j.redox.2021.101959.

[19] J.R. Riddell, X.Y. Wang, H. Minderman, S.O. Gollnick, Peroxiredoxin 1 stimulates secretion of proinflammatory cytokines by binding to TLR4 184, J Immunol, Baltimore, Md, 1950, pp. 1022–1030, https://doi.org/10.4049/jimmunol.0901945, 2010.

[20] T. Shichita, et al., Peroxiredoxin family proteins are key initiators of post-ischemic inflammation in the brain, Nat. Med. 18 (2012) 911–917, https://doi.org/10.1038/nm.2749.

[21] R. Yanagisawa, et al., Peroxiredoxin I null mice exhibits reduced acute lung inflammation following ozone exposure, J. Biochem. 152 (2012) 595–601, https://doi.org/10.1093/jb/mvs113.

[22] G. Chu, et al., Identification and verification of PRDX1 as an inflammation marker for colorectal cancer progression, Am J Transl Res 8 (2016) 842–859.

[23] Q. Liu, Y. Zhang, PRDX1 enhances cerebral ischemia-reperfusion injury through activation of TLR4-regulated inflammation and apoptosis, Biochem. Biophys. Res. Commun. 519 (2019) 453–461, https://doi.org/10.1016/j.bbrc.2019.08.077.

[24] C.H. Liu, et al., Peroxiredoxin 1 induces inflammatory cytokine response and predicts outcome of cardiogenic shock patients necessitating extracorporeal membrane oxygenation: an observational cohort study and translational approach, J. Transl. Med. 14 (2016) 114, https://doi.org/10.1186/s12967-016-0869-x.

[25] A. Pachot, J.L. Blond, B. Mougin, P. Miossec, Peptidylpropyl isomerase B (PPIB): a suitable reference gene for mRNA quantification in peripheral whole blood, J. Biotechnol. 114 (2004) 121–124, https://doi.org/10.1016/j.jbiotec.2004.07.001.

[26] J.M. Bland, D.G. Altman, Calculating correlation coefficients with repeated observations: Part 1–Correlation within subjects, BMJ 310 (1995) 446, https://doi.org/10.1136/bmj.310.6977.446.

[27] I. Levy, et al., Nosocomial infections after cardiac surgery in infants and children: incidence and risk factors, J. Hosp. Infect. 53 (2003) 111–116, https://doi.org/10.1053/jhin.2002.1359.

[28] S.O. Algra, et al., Bedside prediction rule for infections after pediatric cardiac surgery, Intensive Care Med. 38 (2012) 474–481, https://doi.org/10.1007/s00134-011-2454-3.

[29] E. Sarvikivi, O. Lyytikäinen, H. Nieminen, H. Sairanen, H. Saxén, Nosocomial infections after pediatric cardiac surgery, Am. J. Infect. Contr. 36 (2008) 564–569, https://doi.org/10.1016/j.ajic.2007.11.006.

[30] A. Pachot, et al., Messenger RNA expression of major histocompatibility complex class II genes in whole blood from septic shock patients, Crit. Care Med. 33 (2005) 31–38, https://doi.org/10.1097/01.ccm.0000150958.20209.a3, discussion 236-237.

[31] W. Lee, et al., Human peroxiredoxin 1 and 2 are not duplicate proteins: the unique presence of CYS83 in Prx1 underscores the structural and functional differences between Prx1 and Prx2, J. Biol. Chem. 282 (2007) 22011–22022, https://doi.org/10.1074/jbc.M610330200.

[32] E. Aksoy, et al., The p110δ isoform of the kinase PI(3)K controls the subcellular compartmentalization of TLR4 signaling and protects from endotoxic shock, Nat. Immunol. 13 (2012) 1045–1054, https://doi.org/10.1038/ni.2426.

[33] J.G. Laffey, J.F. Boylan, D.C. Cheng, The systemic inflammatory response to cardiac surgery: implications for the anesthesiologist, Anesthesiology 97 (2002) 215–252, https://doi.org/10.1097/00000542-200207000-00030.

[34] F. Beyersdorf, The use of controlled reperfusion strategies in cardiac surgery to minimize ischaemia/reperfusion damage, Cardiovasc. Res. 83 (2009) 262–268, https://doi.org/10.1093/cvr/cvp110.

[35] M. Zakkar, G. Guida, M.S. Suleiman, G.D. Angelini, Cardiopulmonary bypass and oxidative stress, Oxid Med Cell Longev (2015), 189863, https://doi.org/10.1155/2015/189863, 2015.

[36] A. Mohammad, et al., A curious case of cysteines in human peroxiredoxin I, Redox Biol 37 (2020), 101738, https://doi.org/10.1016/j.redox.2020.101738.

[37] Y.P. Li, et al., The compromised inflammatory response to bacterial components after pediatric cardiac surgery is associated with cardiopulmonary bypass-suppressed Toll-like receptor signal transduction pathways, J. Crit. Care 29 (2014) 312, https://doi.org/10.1016/j.jcrc.2013.10.008, e317-313.